Infrared absorption of GeNNO isolated in solid Ar

Zih-Min Jiang, Joerg Glatthaar, and Yuan-Pern Lee

Citation: The Journal of Chemical Physics **131**, 144504 (2009); doi: 10.1063/1.3236384
View online: http://dx.doi.org/10.1063/1.3236384
View Table of Contents: http://scitation.aip.org/content/aip/journal/jcp/131/14?ver=pdfcov
Published by the AIP Publishing

Infrared absorption of GeNNO isolated in solid Ar

Zih-Min Jiang,[1] Joerg Glatthaar,[1,a)] and Yuan-Pern Lee[2,b)]
[1]*Department of Applied Chemistry and Institute of Molecular Science, National Chiao Tung University, Hsinchu 30010, Taiwan*
[2]*Department of Applied Chemistry and Institute of Molecular Science, National Chiao Tung University, Hsinchu 30010, Taiwan and Institute of Atomic and Molecular Sciences, Academia Sinica, Taipei 10617, Taiwan*

(Received 12 July 2009; accepted 1 September 2009; published online 8 October 2009)

Codeposition of thermally generated atomic germanium vapor and nitrous oxide (N_2O) in Ar onto a substrate at 11 K produced infrared absorption lines in several sets. The most prominent comprises intense lines at 1443.7, 1102.4, and 784.0 cm^{-1} that become diminished upon irradiation with UV or visible light. These lines are attributed to ν_1 (NO stretching), ν_2 (NN+GeN stretching), and ν_3 (NNO bending+NN stretching) modes of singlet GeNNO. Two additional weak features at 1238.1 and 2859.2 cm^{-1} are assigned as $\nu_3+\nu_4$ and $2\nu_1$ of GeNNO, respectively. Weak doublet features at 1259.3/1255.5 and 1488.9/1486.4 cm^{-1} are tentatively assigned to ν_2 of triplet GeONN and ν_1 of singlet *cyc*-Ge-η^2 [NN(O)], respectively. Quantum-chemical calculations on the Ge+N_2O system with density-functional theory (B3LYP /aug-cc-pVTZ) predict five stable structures: GeNNO (singlet and triplet), singlet *cyc*-Ge-η^2 [NN(O)], triplet *cyc*-Ge-η^2 (NNO), GeONN (singlet and triplet), and singlet GeNON. Vibrational wavenumbers, relative IR intensities, and ^{15}N-isotopic ratios for observed species are consistent with those computed. Irradiation of singlet GeNNO with $\lambda=248$ or 193 nm or $\lambda>525$ nm yields GeO. © *2009 American Institute of Physics*. [doi:10.1063/1.3236384]

I. INTRODUCTION

There is an increased attention to applications of oxides and nitrides of Ge in electronic devices.[1] The greater mobility of carriers in germanium (Ge) than in silicon (Si) has promoted renewed interest in Ge-based high-performance logic devices.[2] SiGe *p* metal-oxide semiconductor field-effect transistor has attracted much attention because of the improved mobility and current drive capability.[3] Si/Ge quantum dots embedded in an insulator have prospective applications not only for silicon-based optoelectronic devices having a large quantum efficiency for light emission[4,5] but also for single-electron transistor memories at ambient temperature.[6,7] With ultrahigh-vacuum chemical vapor deposition, Kim *et al.* demonstrated that annealing with N_2O is an important factor in the formation of Ge dots on insulators.[8] Bera *et al.* also demonstrated that Si/Ge oxide films grown in a N_2O ambient have much improved leakage current, charge to breakdown, and breakdown field over those grown under pure O_2.[9] A fundamental understanding of the reaction between Ge and N_2O is hence important in these processes.

The interactions of N_2O with Ge (111), disordered Ge (111), and amorphous Ge surfaces were studied near 300 K using high-resolution electron energy-loss spectroscopy (EELS), core-level and valence-band EELS, and Auger electron spectroscopy.[10] From these investigations, N_2O molecules were found to decompose into desorbing N_2 molecules and chemisorbed oxygen atoms.

The reported rate coefficients of the gaseous reaction Ge+N_2O range $(1.2-9.9)\times10^{-12}$ cm^3 $molecule^{-1}$ s^{-1} near 298 K[11–14] and $(5.7-7.6)\times10^{-12}$ cm^3 $molecule^{-1}$ s^{-1} near 580 K.[13,15] Hager *et al.*[16] and Capelle and Brom, Jr.[17] detected emission from electronically excited states $a\ ^3\Sigma^+$, $b\ ^3\Pi_1$, and $A\ ^1\Pi$ of GeO, designated GeO*, from reaction of Ge with N_2O. Fontijn and Felder reported that the order of GeO* photon yield was only 10^{-4}.[15] To explain these results, they proposed a mechanism involving a preferential reaction of Ge in its $^3P_1$ state with N_2O to form a "reservoir" GeO** state, from which the emitting GeO* states were produced via collision.

Theoretical calculations on the Ge+N_2O system, which focused on the formation of a GeONN complex and subsequent reactions, have been reported.[18] An argument based on electronic correlations among separated fragments Ge+O+N_2 was proposed to explain the inefficiency of the low-energy adiabatic path from ground-state reactants Ge(^3P)+N_2O($^1\Sigma^+$) to energetically accessible GeO+N_2($^1\Sigma_g^+$) product states. No other reaction channels of the reaction Ge+N_2O have been investigated either experimentally or theoretically.

Naulin *et al.* investigated the reaction of Si+N_2O using laser-induced fluorescence to detect SiN and deduced the existence of the product channel SiN+NO.[19] The reaction intermediate *trans*-SiNNO was observed in a matrix codeposited from Si vapor and a gaseous mixture of N_2O and Ar.[20] One would expect that a similar reaction path also exists for the Ge+N_2O reaction.

From the reaction of laser-ablated Ge with N_2, we reported the production of GeNNGe isolated in solid Ar and its identification with infrared (IR) absorption.[21] Using a similar

a)Permanent address: Department of Organic Chemistry, Justus-Liebig-University Giessen, Heinrich-Buff-Ring 58, D-35392 Giessen, Germany.
b)Author to whom correspondence should be addressed. Electronic mail: yplee@mail.nctu.edu.tw. FAX: 886-3-5713491.

method, we also observed matrix-isolated GeNO and ONGeNO produced from reaction of laser-ablated Ge with NO.[22] As a continuation of our investigation of reactions of Ge with small molecules, we report here the observation of IR absorption of singlet GeNNO and tentatively triplet GeONN and singlet *cyc*-Ge-η^2 [NN(O)], produced from the reaction of Ge with N_2O and their various ^{15}N-labeled species.

II. EXPERIMENTS

The experimental setup is similar to one described previously;[21,22] we provide only brief descriptions here. An oven replaced the laser-ablation setup employed previously to generate gaseous atomic Ge vapor; the design of the oven developed by Maier *et al.* is described elsewhere.[23] Approximately 4–10 mmol of a N_2O/Ar (1/150–1/300) mixture was codeposited with Ge vapor onto a cold Ni-plated Cu substrate for 0.5–1.0 h; the substrate was maintained at 11 K with a closed-cycle refrigerator (expander: Advanced Research Systems, model DE202A; compressor: APD Cryogenics, model HC-4MK).

Several light sources were employed to irradiate the matrix sample to induce photodissociation. Low-pressure and medium-pressure Hg lamps coupled with several optical filters of varied bandpass served as conventional light sources. A KrF excimer laser (248 nm, Lamda Physik, model LPX240i) and an ArF excimer laser (193 nm, Gam laser, model EX100H/60), both operated at 3 Hz with energies ~3 mJ pulse^{-1}, were also employed at various stages of experiments.

IR absorption spectra were recorded with a Fourier-transform IR spectrometer (Bruker, model VERTEX-V80) equipped with a KBr beam splitter and a photovoltaic Hg/Cd/Te detector (77 K) to cover the spectral range 770–4000 cm^{-1}. Typically 200 scans at resolution of 0.5 cm^{-1} were recorded at each stage of experiments.

A thermally shielded boron-nitride crucible (orifice of 3 mm) filled with Ge lumps (~50 mg) was heated resistively with water-cooled electrodes (typical current ~45 A at 5 V) from a dc power supply (Good Will Instek, model PHS-10100A). Under these conditions the surface temperature of the molten Ge was estimated to be ~1430 K. Before the cryogenic compressor was turned on, the oven was slowly preheated to ~1430 K for 2 h until the pressure of the vacuum system dropped below 10^{-5} Torr to remove GeO from the Ge surface and trace adsorbates from the walls, followed by cooling the oven to 298 K before cooling the Ni-plated Cu substrate. After the substrate was cooled down to 11 K, the oven was heated to 1430 K in 3 min.

Gas mixtures of N_2O or its ^{15}N-labeled isotopic variants with Ar (ratio of 1/150–1/300) were prepared with standard techniques. Ar (AGA Gases, 99.995%) was passed through a trap at 77 K to remove traces of water before mixing with N_2O. N_2O (Gas Standards Inc., 99.999%) was purified by degassing at 77 K. Various ^{15}N-labeled N_2O were prepared by heating a solution of the corresponding ^{15}N-labeled ammonium nitrate (NH_4NO_3, ~0.34 g) in concentrated H_2SO_4 (Riedel-de Haën, 95%–97%, 10–15 cm^3) at ~463 K for 1.5 h under 500 Torr of dry N_2.[24] After the reaction, the reagents were cooled to 298 K and the gaseous products were trapped at 77 K. This crude N_2O sample was vaporized and further purified on condensation into a trap originally containing aqueous NaOH (5 cm^3, ~5*M*, thoroughly degassed), followed by three freeze-pump-thaw cycles at 77 K to remove traces of N_2, NO_2, HNO_3, and CO_2. $^{14}NH_4{}^{15}NO_3$, $^{14}NH_4{}^{14}NO_3$, and $^{15}NH_4{}^{15}NO_3$ (Cambridge Isotope Laboratories) have isotopic purities of 98%. Solid Ge (ABCR, Germany, 99.9999%) has a natural isotopic abundance (^{70}Ge:20.38%, ^{72}Ge:27.34%, ^{73}Ge:7.75%, ^{74}Ge:36.71%, ^{76}Ge:7.82%).[25]

III. COMPUTATIONAL METHODS

The equilibrium geometries, energies, vibrational wavenumbers, and IR intensities were computed with the GAUSSIAN 03 program.[26] Our calculations are based on B3LYP density-functional theory (DFT) that uses Becke's three-parameter hybrid exchange functional[27] and the Slater exchange functional with corrections involving a gradient of the density and a correlation functional of Lee, Yang, and Parr, with both local and nonlocal terms.[28] Dunning's correlation-consistent polarized valence triple-zeta basis set augmented with *s*, *p*, *d*, and *f* functions (aug-cc-pVTZ)[29] and the standard split valence 6-311G basis for first-row atoms and the McLean–Chandler (12*s*,9*p*) (631111,52111) basis sets for second-row atoms including *p*, *d*, and diffuse functions [designated 6-311+G(*d*,*p*)] were used.[30,31] For the description of a germanium atom the Wood–Boring quasirelativistic effective core potential[32–34] MWB28 of the Stuttgart/Dresden theoretical group, replacing 28 core electrons by a pseudopotential, was applied. Analytic first and second derivatives were applied for geometry optimization and vibrational wavenumbers at each stationary point.

IV. EXPERIMENTAL RESULTS

A. Reactions of Ge with N_2O

The IR spectrum of a sample of N_2O/Ar (1/300) at 11 K exhibits intense lines at 1282.8 (ν_1) and 2218.6 (ν_3) cm^{-1} and weak lines at 1167.5 ($2\nu_2$), 2459.6 ($\nu_1+2\nu_2$), 2559.2 ($2\nu_1$), 3358.6 ($2\nu_2+\nu_3$), and 3473.6 ($\nu_1+\nu_3$) cm^{-1} due to N_2O; a partial spectrum is shown in trace (a) of Fig. 1. Extremely weak lines of N_2O at 1245.0 (ν_1 of $^{14}N^{14}N^{18}O$), 1878.1/1879.1 ($\nu_1+\nu_2$), 2211.7 (ν_3 of $^{14}N^{14}N^{18}O$), and 2793.0 ($\nu_2+\nu_3$) cm^{-1} were also identified. The two most intense features of N_2O split into multiplets with additional lines at 2227.5, 2226.3, 2224.4, 2222.7, 2215.4, 2214.2, and 2213.0 cm^{-1} for ν_3 and 1287.6, 1286.1, 1278.7, and 1277.7 cm^{-1} for ν_1. The IR spectrum of a sample deposited at 11 K from reaction of atomic Ge vapor with a flowing gaseous mixture of N_2O/Ar (1/300) exhibits a set of new features with intense lines at 1443.7, 1102.4, and 784.0 cm^{-1} and much weaker features at 2859.2, 1488.9/1486.4, 1259.3/1255.5, and 1241.8/1239.7/1238.1 cm^{-1}, as indicated in trace (b) of Fig. 1.

Additional weak features at 2345.1 and 2339.2 cm^{-1} due to CO_2, 2138.4 cm^{-1} due to CO, 2122.9, 2113.9, and

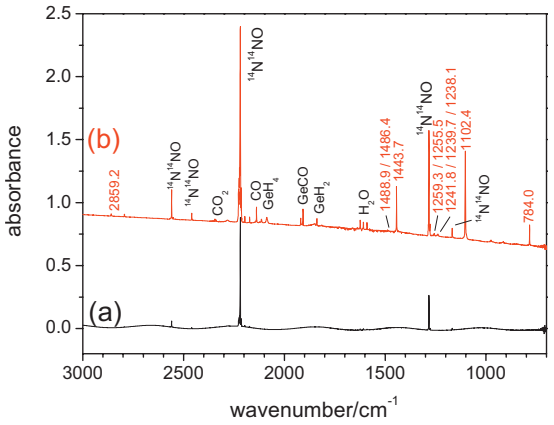

FIG. 1. IR spectra following (a) codeposition at 11 K of a gaseous mixture of N_2O in Ar (1/300) for 5 min and (b) codeposition at 11 K of a gaseous mixture of N_2O in Ar (1/300) with atomic Ge vapor for 1 h. The wavenumbers of new IR signals due to reaction products of Ge and N_2O are listed; the signals of impurities caused by the heating of the crucible are labeled.

2087.4 cm^{-1} due to GeH_4,[35,36] 1919.0 and 1907.6 cm^{-1} due to GeCO,[37–39] 1839.0 and 913.4 cm^{-1} due to GeH_2,[36] 1814.4 due to GeH,[36] 1576.9 cm^{-1} due to GeH_2O,[40] and two unidentified lines at 947.7 and 918.5 cm^{-1} are unrelated to reactions with N_2O because these features were also observed when a stream of Ge atoms was codeposited with pure Ar under similar experimental conditions. These additional features, except the line at 1576.9 cm^{-1} due to GeH_2O, did not change in intensity upon photoirradiation; these additional features remain unaltered in position also when ^{15}N-labeled N_2O was used.

The new features observed from reactions of Ge with N_2O can be organized into several groups according to their photolytic behaviors. Upon irradiation of the matrix with 248-nm laser emission for 5 min or with a medium-pressure Hg lamp combined with a GG525 cutoff filter (pass band $\lambda > 525$ nm) for 2 h, new intense features (group A) at 1443.7, 1102.4, and 784.0 cm^{-1} together with weak lines at 2859.2 (not shown) and 1238.1/1239.7/1241.8 cm^{-1} diminished nearly completely, whereas the quintet lines of GeO near 975 cm^{-1} increased in intensity, as shown in trace (b) of Fig. 2 as a difference spectrum. In these difference spectra, lines

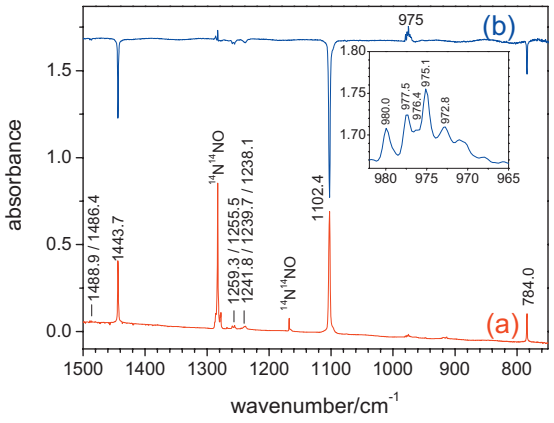

FIG. 2. (a) Partial IR spectrum in the region 750–1500 cm^{-1} recorded after codeposition of Ge and N_2O in Ar (same as trace b of Fig. 1) and (b) difference spectrum after irradiation at 248 nm (KrF laser, 3 Hz, 3.3 mJ $pulse^{-1}$, 5 min).

pointing upwards indicate production, whereas those pointing downwards indicate destruction. The quintet lines observed at 980.0, 977.5, 976.4, 975.1, and 972.8 cm^{-1} correspond to well characterized absorption of GeO with isotopic splitting and relative intensities consistent with natural abundance of Ge isotopes as indicated above,[21,41] except for redshifts of 1.6–1.9 cm^{-1} for the latter due to interactions with nearby N_2. Trace (a) of Fig. 2 is the spectrum of $Ge+N_2O$ in solid Ar before photoirradiation. The weak doublet feature at 1259.3 and 1255.5 cm^{-1} (group B) diminished rapidly only upon irradiation with $\lambda \leq 248$ nm, but its intensity remained unchanged with $\lambda > 525$ nm irradiation. The extremely weak doublet feature at 1488.9 and 1486.4 cm^{-1} (group C) slowly diminished upon irradiation with $\lambda \leq 248$ nm but increased in intensity slightly in the initial ($t < 30$ min) stage of irradiation with $\lambda > 525$ nm, followed by slow decrease in intensity.

The formation of new features upon photolysis at 248 or 254 nm (emission of the low-pressure Hg lamp) is much faster than when 193 nm laser emission was applied. Additional lines at 1863.9 and 1776.3 cm^{-1}, which increased in intensity continuously, are readily assigned as *cis*-N_2O_2;[42,43] they were observed also when N_2O in Ar was deposited at 11 K in the absence of Ge and irradiated under the same conditions. A second group of lines at 1759.1, 1744.9, and 1740.9 cm^{-1} increases rapidly in intensity at the initial stage of irradiation but attained their maximal intensities within 30 min. The first two features are photolysis products of the GeH_2O complex, assigned as HGeO and HGeOH,[40] respectively; the 1740.9 cm^{-1} line is new. These lines did not shift when ^{15}N-labeled N_2O was used. They were also observed when Ge in Ar was deposited in the absence of N_2O and irradiated under the same conditions.

B. Reaction of Ge with ^{15}N-labeled N_2O

When isotopically labeled $^{15}N^{14}NO$ replaced $^{14}N^{14}NO$, the two main lines of $^{14}N^{14}NO$ shifted to 1267.9 (ν_1) and 2196.4 (ν_3) cm^{-1}, and weak features shifted to 1159.6 ($2\nu_2$), 1239.8 (ν_1 of $^{15}N^{14}N^{18}O$), 1860.8/1861.8 ($\nu_1+\nu_2$), 2189.0 (ν_3 of $^{15}N^{14}N^{18}O$), 2530.8 ($2\nu_1$), 2767.5 ($\nu_2+\nu_3$), 3328.4 ($2\nu_2+\nu_3$), and 3436.5 ($\nu_1+\nu_3$) cm^{-1}. Additional multiple lines of the two most intense features of $^{15}N^{14}NO$ are at 2204.9, 2203.9, 2201.3, 2200.0, 2193.1, 2192.1, and 2191.0 (ν_3) cm^{-1} and 1272.4, 1270.4, 1264.0, and 1263.2 (ν_1) cm^{-1}.

Upon reaction with Ge, the new lines in group A shifted to 2850.9, 1440.2, 1231.2/1232.5/1234.5, 1074.7, and 778.7 cm^{-1}. Those in group B shifted to 1244.6 and 1241.8 cm^{-1} and those in group C to 1486.7 and 1484.2 cm^{-1}. A partial difference spectrum upon irradiation at 248 nm is shown in trace (b) of Fig. 3 for comparison with results of $Ge+{}^{14}N^{14}NO$ (trace a); the difference spectra of the matrices upon 248 nm laser irradiation are shown to indicate the species produced (positive lines) or destroyed (negative lines) upon irradiation. The photochemical behaviors of these features are the same as those observed in the $Ge+{}^{14}N^{14}NO$ experiment.

When isotopically labeled $^{14}N^{15}NO$ replaced $^{14}N^{14}NO$, lines of $^{14}N^{14}NO$ shifted to 1143.6 ($2\nu_2$), 1238.3 (ν_1 of

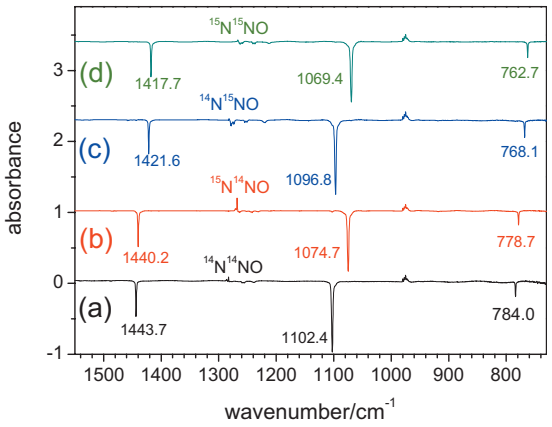

FIG. 3. Difference spectra of matrices codeposited with Ge and various ^{15}N-labeled N_2O upon irradiation at 248 nm: (a) $^{14}N^{14}NO$, (b) $^{15}N^{14}NO$, (c) $^{14}N^{15}NO$, and (d) $^{15}N^{15}NO$.

$^{14}N^{15}N^{18}O$), 1278.2 (ν_1), 1857.9/1858.7 ($\nu_1+\nu_2$), 2166.1 (ν_3 of $^{14}N^{15}N^{18}O$), 2172.5 (ν_3), 2548.1 ($2\nu_1$), 2734.7 ($\nu_2+\nu_3$), 3290.0 ($2\nu_2+\nu_3$), and 3425.0 ($\nu_1+\nu_3$) cm^{-1}. The two most intense fundamentals of $^{14}N^{15}NO$ show additional lines at 2181.5, 2180.3, 2178.4, 2176.9, 2169.7, 2168.5, and 2167.2 (ν_3) cm^{-1}, and 1282.7, 1281.5, 1274.1, and 1272.8 (ν_1) cm^{-1}. Upon reaction with Ge, the new lines in group A shifted to 2816.6, 1421.6, 1219.1/1220.8/1222.7, 1096.8, and 768.1 cm^{-1}, those in group B shifted to 1254.6 and 1250.9 cm^{-1}, and those in group C shifted to 1458.7 and 1456.2 cm^{-1}. A partial difference spectrum upon irradiation at 248 nm is shown in trace (c) of Fig. 3.

When isotopically labeled $^{15}N^{15}NO$ replaced $^{14}N^{14}NO$, lines of $^{14}N^{14}NO$ shifted to 1135.9 ($2\nu_2$), 1224.1 (ν_1 of $^{15}N^{15}N^{18}O$), 1263.2 (ν_1), 1841.1 ($\nu_1+\nu_2$), 2142.4 (ν_3 of $^{15}N^{15}N^{18}O$), 2149.6 (ν_3), 2519.1 ($2\nu_1$), 2708.3 ($\nu_2+\nu_3$), 3259.0 ($2\nu_2+\nu_3$), and 3387.1 ($\nu_1+\nu_3$) cm^{-1}. The most intense fundamentals of $^{15}N^{15}NO$ are split into multiplets with additional lines at 2158.1, 2157.1, 2155.2, 2153.5, 2146.5, 2145.3, and 2144.3 cm^{-1} (ν_3) and 1268.0, 1266.3, 1259.4, and 1258.2 cm^{-1} (ν_1). Upon reaction with Ge, the new lines in group A shifted to 2808.0, 1417.7, 1211.3/1213.1/1215.1, 1069.4, and 762.7 cm^{-1}, those in group B shifted to 1240.6 and 1237.1 cm^{-1}, and those in group C shifted to 1456.4 and 1454.1 cm^{-1}. A partial difference spectrum upon irradiation at 248 nm is shown in trace (d) of Fig. 3.

The observed wavenumbers of these new features from the reaction of Ge with various ^{15}N-labeled N_2O are summarized in Table I. As the positions of lines assigned to GeO remain unaltered when such labeled N_2O were used, they are not listed in Table I.

V. RESULTS OF QUANTUM-CHEMICAL COMPUTATIONS

A. Energies and geometries of GeN_2O isomers

With theoretical calculations according to B3LYP DFT and aug-cc-pVTZ and 6-311+G(d,p) basis sets, we located five isomers of GeN_2O: GeNNO (in singlet and triplet electronic states), *cyc*-^{1}Ge-η^2 [NN(O)], *cyc*-^{3}Ge-η^2 (NNO), GeONN (in singlet and triplet electronic states), and ^{1}GeNON; we indicate singlet and triplet electronic states

TABLE I. Vibrational wavenumbers (cm^{-1}) of new lines observed upon codeposition of Ge vapor with a mixture of N_2O/Ar (1/200) at 11 K.

Group	Species	Mode	$^{14}N^{14}NO$	$^{15}N^{14}NO$	$^{14}N^{15}NO$	$^{15}N^{15}NO$
A	^{1}GeNNO	ν_1	1443.7	1440.2 (0.9976)[a]	1421.6 (0.9847)[a]	1417.7 (0.9820)[a]
		ν_2	1102.4	1074.7 (0.9749)	1096.8 (0.9949)	1069.4 (0.9701)
		ν_3	784.0	778.7 (0.9932)	768.1 (0.9797)	762.7 (0.9728)
		$\nu_3+\nu_4$	1241.8[b]	1234.5[b] (0.9941)	1222.7[b] (0.9846)	1215.1[b] (0.9785)
			1239.7	1232.5 (0.9942)	1220.8 (0.9848)	1213.1 (0.9785)
			1238.1	1231.2 (0.9944)	1219.1 (0.9847)	1211.3 (0.9784)
		$2\nu_1$	2859.2	2850.9 (0.9971)	2816.6 (0.9851)	2808.0 (0.9821)
B	^{3}GeONN	ν_2	1259.3	1244.6 (0.9883)	1254.6 (0.9963)	1240.6 (0.9852)
			1255.5	1241.8 (0.9891)	1250.9 (0.9963)	1237.1 (0.9853)
C	*cyc*-^{1}Ge-η^2 [NN(O)]	ν_1	1488.9	1486.7 (0.9985)	1458.7 (0.9797)	1456.4 (0.9782)
			1486.4	1484.2 (0.9985)	1456.2 (0.9797)	1454.1 (0.9783)

[a]The isotopic ratio, defined as the ratio of vibrational wavenumber of the specific isotopic variant to that of the naturally abundant species containing ^{74}Ge, ^{14}N, and ^{16}O are listed in parentheses.
[b]The first two lines correspond to ^{70}Ge and ^{72}Ge species and the third one to an unresolved contribution of ^{73}Ge and ^{74}Ge species.

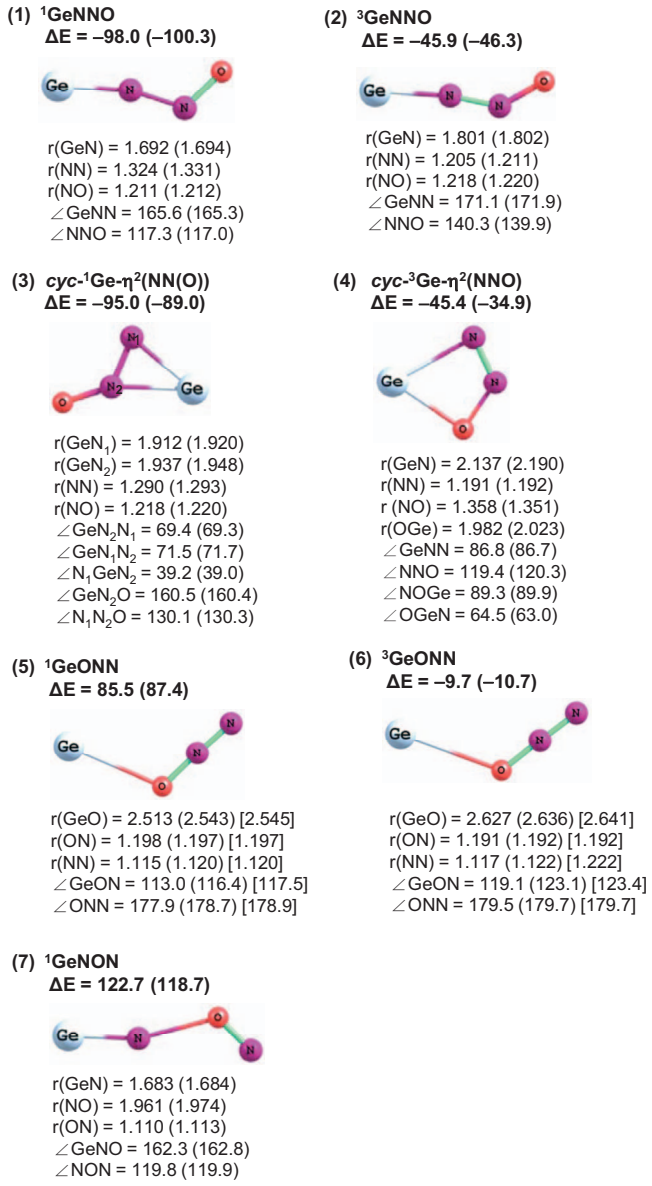

FIG. 4. Geometries and relative energies of stable GeN_2O isomers computed with B3LYP/aug-cc-pVTZ and B3LYP/6-311+G(d,p) methods. Bond lengths are in Å, bond angles in degrees, and relative energies in kJ mol^{-1}. Values derived from B3LYP/6-311+G(d,p) are listed in parentheses. Those reported previously (Ref. 18) using B3LYP/6-311+G* are listed in brackets.

with superscripts "1" and "3," respectively, before "Ge." ^{1}GeONN and ^{1}GeNON are unlikely to be produced from ^{3}Ge+N_2O because they have energies greater than the reactants. Figure 4 shows the geometries and relative energies (zero-point energy corrected) of these isomers, respectively; values from B3LYP/6-311+G(d,p) computations are listed in parentheses. The reference energy is Ge+N_2O at −2261.734 83 hartree for B3LYP/aug-cc-pVTZ or −2261.638 50 hartree for B3LYP/6-311+G(d,p). Energies, zero-point energies, and relative energies of GeN_2O isomers predicted with B3LYP/aug-cc-pVTZ and B3LYP/6-311+G(d,p) are available from the Electronic Physics Auxiliary Publication Service (EPAPS).[44]

According to computations with B3LYP/aug-cc-pVTZ, the planar ^{1}GeNNO has the least energy, −98.0 kJ mol^{-1}, relative to Ge+N_2O. The N–O bond length is 1.211 Å, slightly greater than that of NO (1.151 Å).[45] The Ge–N bond length of 1.692 Å is slightly smaller than those for GeNO (1.785 Å) (Ref. 22) predicted at BLYP/aug-cc-pVTZ and GeNNGe (1.709 Å) (Ref. 21) predicted at B3LYP/aug-cc-pVTZ. The N–N bond length of 1.324 Å is 0.084 Å greater than that of GeNNGe (1.240 Å) predicted at the same level of theory.[21]

The ground electronic state of GeNNO is singlet ($^1A'$); its electronically excited triplet state ($^3A''$) lies 52.1 kJ mol^{-1} above the ground state. The main difference in geometry between ^{1}GeNNO and ^{3}GeNNO is that the ONN moiety of the latter is less bent and the length of the N–N bond decreases from 1.324 Å in the ground singlet state to 1.205 Å in its triplet state, and the length of the Ge–N bond increases from 1.692 to 1.801 Å.

The planar C_s-symmetric cyc-^{1}Ge-η^2 [NN(O)], with Ge and two N atoms forming a three-membered ring, has energy of −95.0 kJ mol^{-1}, slightly greater than that of ^{1}GeNNO. The two Ge–N bonds in the slightly asymmetric three-membered ring are 1.912 (Ge−N_1) and 1.937 Å (Ge−N_2), indicating a slightly stronger bond of Ge to the terminal nitrogen of the NNO moiety. The GeN_2 ring is stabilized via an electron-withdrawing (−I) effect of the oxygen substituent at N_2. Both Ge–N bonds are shorter than the computed bond length of 2.023 Å for Ge–N bonds in cyc-GeN_2,[21] whereas the N–N bond length of 1.290 Å is much larger than the N–N bond in cyc-GeN_2 (1.195 Å). The NGeN angle of 39.2° is larger than the NGeN angle of 34.4° in cyc-GeN_2.

On the corresponding triplet energy surface, cyc-^{3}Ge-η^2 (NNO) has energy of −45.4 kJ mol^{-1} below Ge+N_2O, similar to that of ^{3}GeNNO. The NNO moiety is bent (119.4°) with elongated N–N (1.191 Å) and N–O (1.358 Å) bonds relative to free NNO (N–N: 1.125 Å, N–O: 1.185 Å).

^{3}GeONN(^{3}A) with energy of −9.7 kJ mol^{-1} relative to Ge+N_2O may be considered as a complex with ^{3}Ge attaching the O atom of N_2O. The Ge–O bond length of 2.627 Å, the GeON bond angle of 119.1°, and the almost linear ONN moiety indicate a weak interaction between ^{3}Ge and the O atom. The N–O bond length of 1.191 Å is slightly longer than the N–O bond in NNO (1.185 Å). The N–N bond length of 1.117 Å is 0.008 Å shorter than that for NNO (1.125 Å) predicted at the B3LYP/aug-cc-pVTZ level.

The singlet electronically excited state of GeONN, ^{1}GeONN, may be considered as a complex with ^{1}Ge attaching the O atom of N_2O; its energy is 85.5 kJ mol^{-1} above ^{3}Ge+N_2O. The Ge–O bond length of 2.513 Å, the GeON bond angle of 113.0°, and the almost linear (177.9°) ONN moiety indicates a slightly stronger interaction between ^{1}Ge and the O atom in ^{1}GeONN relative to that between ^{3}Ge and O in ^{3}GeONN (Ge–O, length of 2.627 Å). Previous computations[18] on both singlet and triplet states of GeONN using B3LYP/6-311+G*, listed in brackets in Fig. 4, are consistent with our results.

GeNON ($^1A'$) is the least stable isomer of GeN_2O, with energy of 122.7 kJ mol^{-1} above ^{3}Ge+N_2O. The Ge–N bond length of 1.683 Å is slightly shorter than that of ^{1}GeNNO (1.692 Å). The terminal N–O bond length of 1.110 Å is 0.1

Å shorter than that of ^{1}GeNNO, whereas the central N–O bond length of 1.961 Å indicates weak bonding between the GeN and NO moieties.

B. Vibrational wavenumbers and IR Intensities of GeN_2O isomers

Vibrational wavenumbers and IR intensities for each isomer calculated with B3LYP/aug-cc-pVTZ and B3LYP/6-311+G(d,p) are listed in Table II. For ^{1}GeNNO, two intense IR absorption lines at 1511 (ν_1, NO stretch) and 1165 (ν_2, NN+GeN stretch) cm^{-1} and a weaker absorption at 773 (ν_3, NNO bend+NN stretch) cm^{-1} are predicted. The force constant of 11.6 mdyne Å^{-1} for the Ge–N bond indicates some double-bond character. For ^{3}GeNNO, two intense IR lines of similar intensities at 1712 (ν_1, NNO *a*-stretch) and 1186 (ν_2, NNO *s*-stretch) cm^{-1} are within the range of our detection. The weaker interaction of the Ge atom with the terminal nitrogen of the NNO moiety in ^{3}GeNNO produces blueshifts of these two lines compared with ^{1}GeNNO.

cyc-^{1}Ge-η^2 [NN(O)] is predicted to show an intense absorption near 1550 cm^{-1} (ν_1, NO stretch). The other absorption lines within the range of our detection are predicted to be weak. Because of the increased bond length, the N–N stretching mode is red-shifted to 1190 cm^{-1} for comparison with *cyc*-GeN_2 (1662 cm^{-1}).[21] In contrast, *cyc*-^{3}Ge-η^2 (NNO) is predicted to show an intense line at 1654 cm^{-1} (ν_1, NN stretch) and a medium one at 847 cm^{-1} (ν_2, NO stretch).

^{3}GeONN and ^{1}GeONN are expected to have similar IR absorption patterns. In the range of our detection, lines at 2346 (ν_1, NNO *a*-stretch) and 1296 (ν_2, NNO *s*-stretch) cm^{-1} are predicted for ^{3}GeONN, and 2347 (ν_1) and 1257 (ν_2) cm^{-1} for ^{1}GeONN. The blueshift of the ν_1 mode and the redshift of the ν_2 mode compared with free N_2O (ν_1 =2306.7 cm^{-1} and ν_2=1314.1 cm^{-1}) are consistent with the changes in the geometry of the ONN moiety due to the complex formation with the Ge atom.

For GeNON, two intense vibrational modes are predicted at 2000 (ν_1, NO stretch) and 977 (ν_2, GeN stretch) cm^{-1}. The NO stretch is blueshifted relative to free NO (1968 cm^{-1}) by 32 cm^{-1}, and the GeN stretch is blueshifted by 26 cm^{-1} relative to free GeN (951 cm^{-1}). Both effects are explicable according to a slightly positive charge of the NO moiety, causing a larger force constant (35.0 versus 33.9 mdyne Å^{-1} for free NO) and by the slightly negatively charged GeN moiety, causing a stronger attraction between Ge and N atoms (force constant of 8.84 versus 8.57 mdyne Å^{-1} for free GeN).

Vibrational wavenumbers of these species containing one or two ^{15}N or one ^{72}Ge were also computed and presented as isotopic ratios in Table II. The isotopic ratio is defined as the ratio of vibrational wavenumber of the specific isotopic variant to that of the naturally abundant species, in this case, species containing ^{74}Ge, ^{14}N, and ^{16}O.

C. Reaction paths of $Ge+N_2O$

Reaction paths and energies of the transition states and stable species on the GeN_2O potential energy surface computed with B3LYP/aug-cc-pVTZ are shown in Fig. 5. Computed energies and geometries of relevant transition states TS1–TS8 are available from the EPAPS.[44] When ^{3}Ge and N_2O approach closely, at least six scenarios might be considered. The Ge atom might interact with the terminal oxygen atom, the terminal nitrogen, or the central nitrogen atom of N_2O. Alternatively, the Ge atom might interact simultaneously with two nitrogen atom or the oxygen atom and one nitrogen atom in either the central or terminal position.

Interaction between the oxygen atom and the Ge atom is slightly attractive; with no activation a ^{3}GeONN complex is formed. ^{3}GeONN is further connected via TS1 (E_A =22.0 kJ mol^{-1}) to a reaction path forming ^{3}GeO and N_2. The TS1 transition state having a *trans*-like structure is more than 10 kJ mol^{-1} lower in energy at the B3LYP/6-311+G(d,p) level of theory than the transition state with a *cis*-like structure that was reported previously by Wang *et al.*[18] This *cis*-like transition state has a structure almost identical to TS2 (see Fig. S1 in EPAPS); TS2 connects between ^{3}Ge+N_2O and *cyc*-^{3}Ge-η^2 (NNO) but not connects to the reaction pathway leading to ^{3}GeO and N_2. All considerations and conclusion derived based on this transition state in Ref. 18 might be in error.

Interaction between the terminal nitrogen of N_2O and ^{3}Ge is strongly exothermic yielding with no activation directly a stable ^{3}GeNNO complex with a short GeN bond length of 1.801 Å. In contrast, interaction between the central nitrogen atom and ^{3}Ge is repulsive, even if the initial NNO skeleton geometry is slightly bent. During the optimization the Ge atom becomes oriented toward the terminal nitrogen but eventually forms the stable ^{3}GeNNO.

The same argument is applicable for the interaction between ^{3}Ge and the two neighboring nitrogen atoms. No stable triplet structure containing a three-membered GeNN ring was located. The bond between the central nitrogen and the germanium atom opened and the structure collapsed into the more stabilized ^{3}GeNNO. The most important reaction channel of ^{3}GeNNO occurs on intersystem crossing to the more stable ^{3}GeNNO (−98.0 kJ mol^{-1}); the two structures are similar. The path to generate GeN and NO from ^{3}GeNNO has a high barrier via transition state TS5 at 133.7 kJ mol^{-1}.

Interaction between ^{3}Ge and both terminal nitrogen and oxygen atoms is an endothermic process, because the NNO unit must become bent to accomplish a doubly stabilizing interaction between Ge, O, and N atoms. Transition state TS2 forming *cyc*-^{3}Ge-η^2 (NNO) has energy of 25.5 kJ mol^{-1} greater than the initial ^{3}Ge+N_2O. *cyc*-Ge-$^3\eta^2$ (NNO) is further connected to ^{3}GeNNO (−45.9 kJ mol^{-1}) via transition state TS3 with a barrier of 36.4 kJ mol^{-1}. A third transition state TS4 (−37.7 kJ mol^{-1}) with a barrier of 7.7 kJ mol^{-1} leads to the formation of ^{3}GeO and N_2.

^{3}GeNNO has several reaction channels. It might dissociate to form GeO+N_2 via a *s-cis* symmetric transition state TS6 located at −46.3 kJ mol^{-1}; the barrier of 51.7 kJ mol^{-1} represents the smallest among known reaction paths of ^{1}GeNNO. A second transition state TS7 at energy −30.8 kJ mol^{-1} precedes formation of *cyc*-^{1}Ge-η^2 [NN(O)]; the GeNN angle decreases from 165.6° to 99.1°. The reaction path leading to ^{1}GeNON via transition state TS8 (162.8 kJ mol^{-1}) exhibits a large barrier.

TABLE II. Vibrational wavenumbers (σ), IR intensities (km mol^{-1}), and isotopic ratios of seven stable species of GeN_2O predicted with B3LYP/aug-cc-pVTZ and B3LYP/6-311+G(d,p).

			Absorption		Isotopic ratio[a]			
ν_i	Symmetry	Mode	σ (cm^{-1})	IR intensities	$^{15}N^{14}NO$	$^{14}N^{15}NO$	$^{15}N^{15}NO$	^{72}Ge
(1) ^{1}GeNNO								
ν_1	A'	NO stretch	1510.6	243.5	0.9984	0.9842	0.9824	1.0000
			(1523.5)[b]	(258.2)[b]	(0.9985)[b]	(0.9841)[b]	(0.9823)[b]	(1.0000)[b]
ν_2	A'	NN+GeN stretch	1165.4	454.7	0.9726	0.9952	0.9681	1.0006
			(1159.2)	(479.1)	(0.9726)	(0.9953)	(0.9680)	(1.0006)
ν_3	A'	NNO bend+NN stretch	772.5	19.0	0.9935	0.9783	0.9717	1.0002
			(778.1)	(26.5)	(0.9935)	(0.9785)	(0.9719)	(1.0002)
ν_4	A'	GeN stretch+GeNN bend	465.0	6.4	0.9972	0.9908	0.9882	1.0042
			(460.7)	(7.1)	(0.9974)	(0.9908)	(0.9883)	(1.0042)
ν_5	A'	GeNN bend	133.5	6.1	0.9792	0.9985	0.9779	1.0009
			(130.7)	(7.3)	(0.9792)	(0.9986)	(0.9779)	(1.0009)
ν_6	A''	Out-of-plane deformation	118.0	5.4	0.9715	0.9970	0.9684	1.0005
			(125.0)	(7.3)	(0.9716)	(0.9970)	(0.9684)	(1.0005)
(2) ^{3}GeNNO								
ν_1	A'	NNO *a*-stretch	1712.2	257.4	0.9932	0.9781	0.9710	1.0000
			(1714.7)	(262.1)	(0.9933)	(0.9780)	(0.9711)	(1.0000)
ν_2	A'	NNO *s*-stretch	1185.7	274.8	0.9840	0.9968	0.9809	1.0000
			(1185.2)	(274.3)	(0.9841)	(0.9967)	(0.9807)	(1.0000)
ν_3	A'	NNO bend	621.0	80.6	0.9916	0.9798	0.9716	1.0009
			(620.7)	(77.7)	(0.9916)	(0.9797)	(0.9716)	(1.0009)
ν_4	A'	GeN stretch+NNO bend	350.1	1.7	0.9935	0.9932	0.9868	1.0041
			(346.4)	(2.2)	(0.9933)	(0.9934)	(0.9868)	(1.0042)
ν_5	A'	GeNN bend	113.4	1.7	0.9785	0.9983	0.9771	1.0004
			(109.1)	(2.5)	(0.9785)	(0.9984)	(0.9772)	(1.0004)
ν_6	A''	Out-of-plane deformation	175.0	5.8	0.9722	0.9959	0.9680	1.0009
			(185.8)	(7.1)	(0.9728)	(0.9950)	(0.9676)	(1.0009)
(3) *cyc*-^{1}Ge-η^2 [NN(O)]								
ν_1	A'	NO stretch	1549.7	450.8	0.9989	0.9785	0.9775	1.0000
			(1558.5)	(459.1)	(0.9989)	(0.9786)	(0.9776)	(1.0000)
ν_2	A'	NN stretch	1190.2	18.9	0.9822	0.9881	0.9698	1.0000
			(1193.9)	(20.0)	(0.9823)	(0.9880)	(0.9699)	(1.0000)
ν_3	A'	NNO bend	795.0	22.7	0.9836	0.9932	0.9765	1.0001
			(790.5)	(24.0)	(0.9839)	(0.9928)	(0.9764)	(1.0001)
ν_4	A'	GeNN *s*-stretch	526.0	20.5	0.9867	0.9906	0.9781	1.0037
			(513.9)	(20.2)	(0.9863)	(0.9909)	(0.9780)	(1.0037)
ν_5	A'	GeNN bend	300.3	12.1	0.9933	0.9932	0.9868	1.0025
			(293.6)	(11.9)	(0.9933)	(0.9932)	(0.9868)	(1.0025)
ν_6	A''	Out-of-plane deformation	422.5	2.0	0.9992	0.9741	0.9733	1.0002
			(413.6)	(1.7)	(0.9991)	(0.9741)	(0.9733)	(1.0002)
(4) *cyc*-^{1}Ge-η^2 (NNO)								
ν_1	A'	NN stretch	1654.4	201.3	0.9831	0.9835	0.9663	1.0000
			(1682.2)	(199.3)	(0.9831)	(0.9835)	(0.9662)	(1.0000)
ν_2	A'	NO stretch	847.3	52.8	0.9978	0.9900	0.9877	1.0001
			(861.0)	(60.1)	(0.9977)	(0.9898)	(0.9875)	(1.0000)
ν_3	A'	NNO bend	660.7	26.2	0.9885	0.9804	0.9692	1.0001
			(655.8)	(25.8)	(0.9887)	(0.9804)	(0.9694)	(1.0001)
ν_4	A'	GeO stretch	360.9	10.6	0.9988	0.9994	0.9981	1.0030
			(329.2)	(11.4)	(0.9992)	(0.9993)	(0.9984)	(1.0033)
ν_5	A'	GeN stretch	250.0	1.5	0.9803	0.9961	0.9768	1.0035
			(214.5)	(1.9)	(0.9798)	(0.9964)	(0.9766)	(1.0031)
ν_6	A''	Out-of-plane deformation	429.7	5.4	0.9913	0.9824	0.9736	1.0002
			(417.3)	(4.6)	(0.9916)	(0.9822)	(0.9736)	(1.0002)

TABLE II. (*Continued.*)

ν_i	Symmetry	Mode	Absorption σ (cm^{-1})	Absorption IR intensities	Isotopic ratio[a] $^{15}N^{14}NO$	$^{14}N^{15}NO$	$^{15}N^{15}NO$	^{72}Ge
(5) ^{3}GeONN								
ν_1	A'	NNO *a*-stretch	2345.9	461.6	0.9889	0.9790	0.9675	1.0000
			(2349.3)	(495.3)	(0.9891)	(0.9789)	(0.9676)	(1.0000)
ν_2	A'	NNO *s*-stretch	1295.8	113.9	0.9881	0.9979	0.9864	1.0000
			(1302.1)	(110.4)	(0.9879)	(0.9981)	(0.9863)	(1.0000)
ν_3	A'	NNO bend	601.4	3.3	0.9943	0.9773	0.9715	1.0000
			(576.8)	(3.0)	(0.9944)	(0.9773)	(0.9716)	(1.0000)
ν_4	A'	GeO stretch	115.6	8.0	0.9969	0.9974	0.9942	1.0022
			(114.1)	(6.5)	(0.9970)	(0.9970)	(0.9939)	(1.0024)
ν_5	A'	GeON bend	56.4	0.2	0.9842	0.9951	0.9797	1.0035
			(53.7)	(0.2)	(0.9832)	(0.9957)	(0.9791)	(1.0031)
ν_6	A''	Out-of-plane deformation	593.6	4.2	0.9939	0.9771	0.9709	1.0000
			(559.5)	(5.9)	(0.9940)	(0.9771)	(0.9710)	(1.0000)
(6) ^{1}GeONN								
ν_1	A'	NNO *a*-stretch	2346.8	390.9	0.9884	0.9793	0.9673	1.0000
			(2353.5)	(390.0)	(0.9886)	(0.9791)	(0.9674)	(1.0000)
ν_2	A'	NNO *s*-stretch	1256.7	82.5	0.9884	0.9976	0.9865	1.0000
			(1275.9)	(110.6)	(0.9883)	(0.9977)	(0.9864)	(1.0000)
ν_3	A'	NNO bend	527.5	52.5	0.9936	0.9784	0.9718	1.0000
			(510.1)	(24.7)	(0.9936)	(0.9780)	(0.9715)	(1.0000)
ν_4	A'	GeO stretch	146.8	17.9	0.9951	0.9982	0.9931	1.0015
			(140.5)	(16.7)	(0.9966)	(0.9976)	(0.9941)	(1.0020)
ν_5	A'	GeON bend	59.5	0.0	0.9878	0.9931	0.9813	1.0044
			(58.5)	(0.0)	(0.9860)	(0.9941)	(0.9805)	(1.0038)
ν_6	A''	Out-of-plane deformation	586.0	3.1	0.9938	0.9770	0.9707	1.0000
			(556.4)	(5.2)	(0.9939)	(0.9771)	(0.9708)	(1.0000)
(7) ^{1}GeNON								
ν_1	A'	Terminal NO stretch	2000.2	1305.7	1.0000	0.9819	0.9819	1.0000
			(2014.6)	(1337.8)	(1.0000)	(0.9819)	(0.9819)	(1.0000)
ν_2	A'	GeN stretch	976.8	261.7	0.9711	1.0000	0.9711	1.0019
			(968.5)	(252.5)	(0.9710)	(1.0000)	(0.9710)	(1.0018)
ν_3	A'	NON bend	496.1	52.8	0.9957	0.9919	0.9876	1.0001
			(487.1)	(52.5)	(0.9958)	(0.9920)	(0.9878)	(1.0001)
ν_4	A'	Central NO stretch	231.7	30.4	0.9991	0.9846	0.9837	1.0032
			(231.8)	(26.9)	(0.9992)	(0.9844)	(0.9836)	(1.0032)
ν_5	A'	GeNO bend	37.4	21.3	0.9751	0.9953	0.9704	1.0008
			(30.6)	(25.7)	(0.9746)	(0.9961)	(0.9708)	(1.0010)
ν_6	A''	Out-of-plane deformation	12.8	25.5	0.9886	0.9738	0.9627	1.0018
			(36.3)	(31.0)	(0.9729)	(0.9943)	(0.9670)	(1.0002)

[a]The isotopic ratio is defined as the ratio of vibrational wavenumber of the specific isotopic variant to that of the naturally abundant species, in this case, species containing ^{74}Ge, ^{14}N, and ^{16}O.
[b]Values calculated with B3LYP/6-311+G(*d*,*p*) are listed in parentheses.

In summary, the results of computations indicate that reactions of ^3Ge with N_2O likely lead to formation of ^3GeONN and ^3GeNNO; the latter is expected to relax to ^1GeNNO under low-temperature matrix conditions. Other isomers such as ^1GeNON or *cyc*-^3Ge-η^2 (NNO) are unlikely to be produced because the reaction must overcome a large barrier. *cyc*-^3Ge-η^2 (NNO) might not be observed because the barrier for the decay into $^3GeO+N_2$ is small. The probability to produce *cyc*-^1Ge-η^2 [NN(O)] directly in experiments with codeposition of $^3Ge+N_2O$ might be small because we are unable to locate any direct path connecting $^3Ge+N_2O$ with *cyc*-^1Ge-η^2 [NN(O)].

VI. DISCUSSION

A. Assignment of observed new features in group A to ^{1}GeNNO

From the ^{15}N-isotopic substitution experiments (Fig. 3), the new species clearly contains two N atoms; all three main vibrational lines near 1443.7, 1102.4, and 784.0 cm^{-1} involve inequivalent motions from these two N atoms because no observed isotopic shift is identical. The possibility of this species being GeNN is readily excluded because we expect a much larger vibrational wavenumber for the N=N stretching mode of GeNN, as confirmed from quantum-chemical

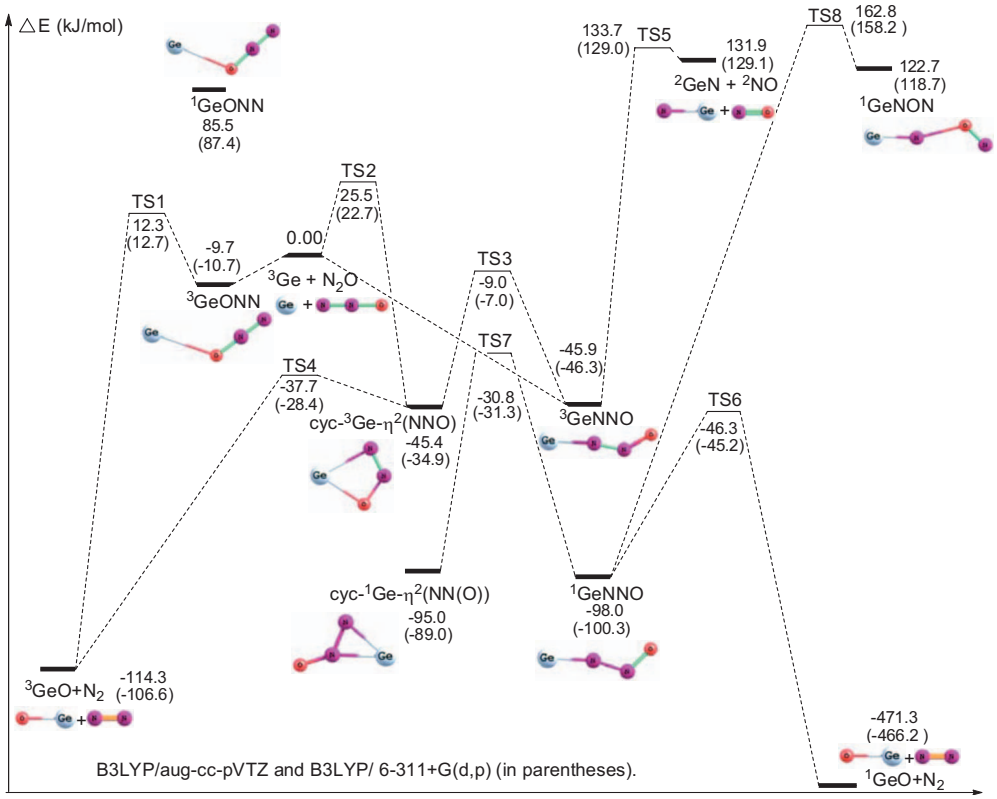

FIG. 5. GeN_2O potential energy computed with B3LYP/aug-cc-pVTZ and B3LYP/6-311+G(d,p) methods. Relative energies are in kJ mol^{-1}; those derived with B3LYP/6-311+G(d,p) are listed in parentheses.

calculations;[21] other isomers of GeN_2, *cyc*-GeN_2, and NGeN have equivalent N atoms and vibrational wavenumbers unmatched with our observation. Hence, the likely carrier of these new features is expected to be one isomer of GeN_2O.

By comparison with computed vibrational wavenumbers listed in Table II, only two candidates have a vibrational mode with wavenumbers similar to our observation: ^{1}GeNNO (1511, 1165, and 773 cm^{-1} from B3LYP/aug-cc-pVTZ) and *cyc*-^{1}Ge-η^2 [NN(O)] (1550, 1190, and 795 cm^{-1}); other isomers have corresponding vibrational wavenumbers predicted to be at least 210 cm^{-1} greater than the observed value. However, the IR intensity distributions differ markedly for these two species. ^{1}GeNNO is predicted to have two intense lines, with that near 1165 cm^{-1} nearly twice as intense as that near 1511 cm^{-1}. In contrast, the line at 1550 cm^{-1} for *cyc*-^{1}Ge-η^2 [NN(O)] is more than 20 times as intense as other lines. Our observed relative intensities of lines at 1443.7 and 1102.4 cm^{-1} (Figs. 2 and 3) are consistent with those predicted for ^{1}GeNNO.

The ^{15}N-isotopic ratios provide further support for the assignments to ^{1}GeNNO. The isotopic ratio is defined as the ratio of vibrational wavenumber of the specific isotopic variant to that of the naturally abundant species, in this case, species containing ^{74}Ge, ^{14}N, and ^{16}O. Observed isotopic ratios are listed parenthetically in Table I to compare with those derived from quantum-chemical calculations in Table II; they agree satisfactorily with those of ^{1}GeNNO, with deviations less than 0.0023. The agreement is much worse for *cyc*-^{1}Ge-η^2 [NN(O)] with deviations as much as 0.0135. Computations predict a shift of the ν_3 line of *cyc*-^{1}Ge-η^2 [^{14}N^{15}N(O)] much smaller than *cyc*-^{1}Ge-η^2 [^{15}N^{14}N(O)], but our observation indicates the reverse.

For convenience, we also list observed and computed isotopic shifts in Table III. We assign the line at 1443.7 cm^{-1} to ν_1 of ^{1}GeNNO; the vibrational wavenumber is consistent with a NO-stretching mode. The observed ^{15}N-isotopic shifts indicate that mainly the central N atom of the NNO moiety is involved in this vibration because these lines observed from reactions of Ge with ^{14}N^{15}NO and ^{15}N^{15}NO show shifts ($\Delta\nu$=−22.1 and −26.0 cm^{-1}, respectively) much greater than that ($\Delta\nu$=−3.5 cm^{-1}) with ^{15}N^{14}NO.

We assign the line at 1102.4 cm^{-1} to the ν_2 mode of ^{1}GeNNO. The observed ^{15}N-isotopic shifts indicate that this vibration mainly involves the terminal N atom rather than the central N atom of the NNO moiety because lines near 1102 cm^{-1} observed from reactions of Ge with ^{15}N^{14}NO and ^{15}N^{15}NO show shifts ($\Delta\nu$=−27.7 and −33.0 cm^{-1}, respectively) much greater than that ($\Delta\nu$=−5.6 cm^{-1}) with ^{14}N^{15}NO. As the GeN stretching mode is expected to show a smaller wavenumber like that predicted at 868.5 cm^{-1} for H_2GeNH,[46] this observed mode must be mixed with NN stretching. If only GeN stretch were involved in this mode, we would expect to observe splitting due to Ge isotopes. The vector displacements computed for this mode confirm this mixing. According to the computations, the absorption lines of the ^{74}Ge- and ^{72}Ge-isotopic species shift by only −0.7 cm^{-1}, not enough for us to resolve these lines. The unresolved Ge-isotopic variants might be the cause of a

TABLE III. Comparison of observed isotopic shifts with those predicted for isomers of GeN_2O with B3LYP/aug-cc-pVTZ and B3LYP/6-311+G(d,p).

Species	ν_i observed		σ [a] (cm^{-1})	Isotopic shift		
				$^{15}N^{14}NO$	$^{14}N^{15}NO$	$^{15}N^{15}NO$
^{1}GeNNO	ν_1	Expt.	1443.7	−3.5	−22.1	−26.0
		Calc.	1510.6	−2.4	−23.9	−26.7
			(1523.5)[b]	(−2.3)[b]	(−24.3)[b]	(−26.9)[b]
	ν_2	Expt.	1102.4	−27.7	−5.6	−33.0
		Calc.	1165.4	−31.9	−5.5	−37.2
			(1159.2)	(−31.8)	(−5.5)	(−37.1)
	ν_3	Expt.	784.0	−5.3	−15.9	−21.3
		Calc.	772.5	−5.0	−16.8	−21.8
			(778.1)	(−5.1)	(−16.7)	(−21.9)
	$\nu_3+\nu_4$	Expt.	1241.8	−7.3	−19.1	−26.7
			1239.7	−7.2	−18.9	−26.6
			1238.1	−7.3	−18.8	−26.6
		Calc.	1237.5	−6.3	−21.1	−27.3
			(1238.8)	(−6.3)	(−21.0)	(−27.2)
	$2\nu_1$	Expt.	2859.2	−8.3	−42.6	−51.2
		Calc.	3021.2	−4.8	−47.7	−53.3
			(3047.0)	(−4.5)	(−48.6)	(−53.8)
^{3}GeONN	ν_2	Expt.	1259.3	−14.7	−4.7	−18.7
			1255.5	−13.7	−4.6	−18.4
		Calc.	1295.8	−15.4	−2.7	−17.6
			(1302.1)	(−15.8)	(−2.5)	(−17.8)
cyc-^{1}Ge-η^2 [NN(O)]	ν_1	Expt.	1488.9	−2.2	−30.2	−32.5
			1486.4	−2.2	−30.2	−32.3
		Calc.	1549.7	−1.7	−33.3	−34.9
			(1558.5)	(−1.7)	(−33.3)	(−35.0)

[a]Vibrational wavenumber of the naturally abundant species containing ^{74}Ge, ^{14}N, and ^{16}O.
[b]Values calculated with B3LYP/6-311+G(d,p) are listed in parentheses.

width of 2.7 cm^{-1} for the feature at 1102.4 cm^{-1}, much greater than that (1.2 cm^{-1}) of the feature at 1443.7 cm^{-1}.

The 784.0 cm^{-1} vibration is assigned as mainly the NNO bending (ν_3) mode. The observed ^{15}N-isotopic shifts indicate that this vibration mainly involves the central N atom rather than the terminal one of the NNO moiety because these features observed from reactions of Ge with $^{14}N^{15}NO$ and $^{15}N^{15}NO$ show shifts ($\Delta\nu$=−15.9 and −21.3 cm^{-1}, respectively) much greater than that ($\Delta\nu$ =−5.3 cm^{-1}) with $^{15}N^{14}NO$. From the computed vector displacements, we assign this mode as NNO bend mixed with some NN stretch. The observed vibrational wavenumber of this mode is slightly greater than the computed value of 772.5 cm^{-1}, likely because of negative anharmonicity of the bending mode; a similar trend was observed for SiNNO.[20]

Two additional features near 2859.2 and 1238.1 cm^{-1} were also identified to belong to group A. The line at 2859.2 cm^{-1} is readily assigned to $2\nu_1$, with an anharmonicity of $\omega_e x_e$=14.1 cm^{-1} for $^{74}Ge^{14}N^{14}N^{16}O$. Corresponding lines observed at 2850.9, 2816.6, and 2808.0 cm^{-1} for $Ge^{15}N^{14}NO$, $Ge^{14}N^{15}NO$, and $Ge^{15}N^{15}NO$ (Fig. 6) show ^{15}N-isotopic shifts roughly twice as large as those observed for ν_1, supporting the assignment of this feature to $2\nu_1$.

The feature near 1238.1 cm^{-1} for ^{1}GeNNO and the corresponding features for various ^{15}N substituted species are shown in Fig. 7. The splitting due to ^{70}Ge, ^{72}Ge, and ^{74}Ge is barely resolvable. For $Ge^{14}N^{14}N^{16}O$ they are deconvoluted to have maxima at 1241.8, 1239.7, and 1238.1 cm^{-1}; the two components from ^{73}Ge and ^{76}Ge species are too weak to be discernible. This feature hence involves the GeN stretching mode, which has contributions to the ν_2 and ν_4 modes. From computed harmonic wavenumbers of six vibrational modes of ^{1}GeNNO, this feature at 1238.1 cm^{-1} is readily assigned as the $\nu_3+\nu_4$ combination; ν_3 is observed at 784.0 cm^{-1}, and ν_4 is computed to be near 465 cm^{-1}. Observed ^{15}N-isotopic ratios are consistent with those computed from harmonic

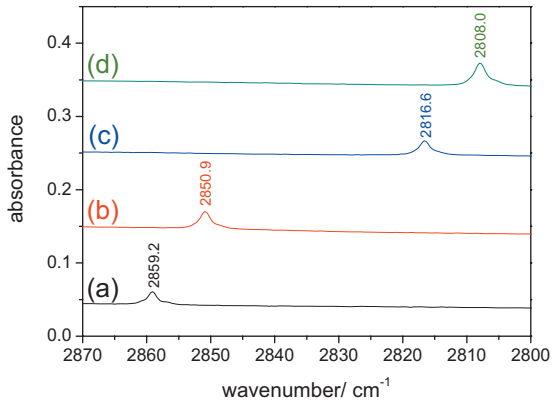

FIG. 6. Partial IR spectrum in the range 2800–2870 cm^{-1} showing absorption of the $2\nu_1$ line of ^{1}GeNNO after codeposition of Ge vapor with various ^{15}N-labeled N_2O: (a) $^{14}N^{14}NO$, (b) $^{15}N^{14}NO$, (c) $^{14}N^{15}NO$, and (d) $^{15}N^{15}NO$.

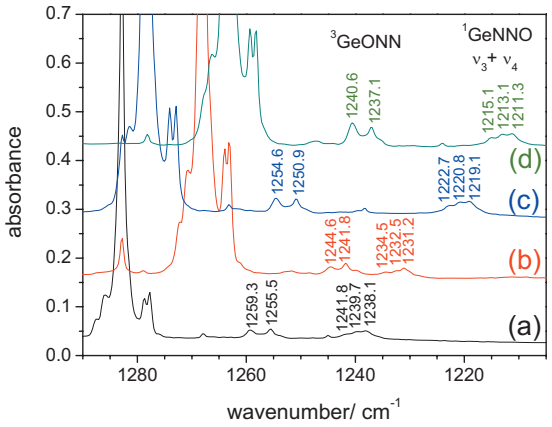

FIG. 7. Partial IR spectrum in the range 1210–1290 cm^{-1} after codeposition of Ge vapor with various ^{15}N-labeled N_2O: (a) $^{14}N^{14}NO$, (b) $^{15}N^{14}NO$, (c) $^{14}N^{15}NO$, and (d) $^{15}N^{15}NO$. The doublets located near the ν_2 fundamental of N_2O are assigned to ^{3}GeONN. The features to the right showing a typical Ge isotope splitting pattern are assigned to the $\nu_3+\nu_4$ lines of ^{1}GeNNO.

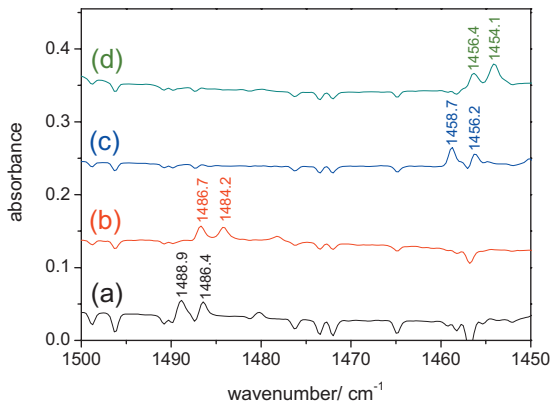

FIG. 8. Partial IR spectrum in the range 1450–1500 cm^{-1} after codeposition of Ge vapor with various ^{15}N-labeled N_2O: (a) $^{14}N^{14}NO$, (b) $^{15}N^{14}NO$, (c) $^{14}N^{15}NO$, and (d) $^{15}N^{15}NO$. The weak doublets are tentatively assigned to *cyc*-^{1}Ge-η^2 [NN(O)].

wavenumbers of the combination. Furthermore, the computed splitting for $\nu_3+\nu_4$ between singlet ^{70}GeNNO and ^{72}GeNNO is 2.2 cm^{-1}, consistent with observed splitting of 2.1 cm^{-1}.

Upon irradiation at 254 nm (low-pressure Hg lamp) or 248 nm (KrF laser), lines of all GeN_2O isomers diminished, and the GeO product was observed. We had hoped to open a second reaction channel by applying the 193 nm emission from an ArF laser, but no indication of the formation of another isomer of GeN_2O or dissociation product such as GeN or NO was observed.

B. Tentative assignment of observed new features in group B to ^{3}GeONN

According to our computations, ^{3}GeONN is expected to be directly formed from ^{3}Ge and N_2O. Notably, the NNO *a*-stretching (ν_1) vibration is predicted to show a blueshift, whereas the NNO *s*-stretching (ν_2) vibration is predicted to show a redshift relative to N_2O. Near the N_2O *s*-stretching vibration of N_2O, a new doublet at 1259.3 and 1255.5 cm^{-1} was observed, as depicted in Fig. 7. No new feature was positively identified near the *a*-stretching region of N_2O, likely because of interference by several extra lines of N_2O caused by the matrix effect.

The only species listed in Table II that has a vibrational band near 1255 cm^{-1} is ^{3}GeONN. Observed ^{15}N-isotopic ratios (Table I) deviate from those computed quantum chemically (Table II) by less than 0.0016. Hence, we tentatively assign this feature to the ν_2 mode of ^{3}GeONN. The reason for the doublet structure is unclear, likely due to different matrix environments.

C. Tentative assignment of observed new features in group C to *cyc*-^{1}Ge-η^2 [NN(O)]

We detected weak signals at 1488.9 and 1486.4 cm^{-1}, as shown in Fig. 8, which belong to neither ^{1}GeNNO nor ^{3}GeONN according to their photochemical behavior. From its photochemical behavior, production with $\lambda > 525$ nm, we derive that this species is closely related to ^{1}GeNNO. These features are tentatively associated with the NO stretching (ν_1) mode of *cyc*-^{1}Ge-η^2 [NN(O)], the second most stable isomer, according to the computed vibrational wavenumbers, IR intensities, and ^{15}N-isotopic ratios. The observed ^{15}N-isotopic ratios (Table I) deviate from those computed quantum chemically (Table II) by less than 0.0012. ν_1 is the only vibrational mode of *cyc*-^{1}Ge-η^2 [NN(O)] that has significant IR intensity for detection.

According to quantum-chemical computations, we found no reaction path that yielded directly *cyc*-^{1}Ge-η^2 [NN(O)] under our experimental conditions. This is consistent with the extremely small intensity observed for this feature.

VII. CONCLUSION

We codeposited Ge metal vapor and N_2O in Ar onto a substrate at 11 K and observed lines in three groups that exhibit distinct photochemical behaviors. The group with the most intense features is assigned to absorption of ^{1}GeNNO; intense lines at 1443.7, 1102.4, and 784.0 cm^{-1} are assigned as ν_1, ν_2, and ν_3, whereas weak lines at 1238.1 and 2859.2 cm^{-1} are assigned as $\nu_3+\nu_4$ and $2\nu_1$, respectively. A weak doublet at 1255.5 and 1259.3 cm^{-1} is tentatively assigned as ν_2 of ^{3}GeONN, and another weak doublet at 1486.4 and 1488.9 cm^{-1} is tentatively assigned to the ν_1 mode of *cyc*-^{1}Ge-η^2 [NN(O)]. Observed vibrational wavenumbers, relative IR intensities, and ^{15}N-isotopic ratios are consistent with those computed quantum chemically. The formation of ^{1}GeNNO is the major channel; Ge reacts with N_2O to form ^{3}GeNNO followed by relaxation to the more stable ^{1}GeNNO.

ACKNOWLEDGMENTS

The National Science Council of Taiwan (Grant No. NSC97-2113-M009-009-MY3) and the MOE-ATU project of the National Chiao Tung University supported this work. The CSC Computing Center at Frankfurt-am-Main provided the resources for quantum-chemical computations. J.G. thanks the National Science Council of Taiwan (Grant No. NSC97-2811-M-009-004) for a visiting professorship.

[1] O. J. Gregory and E. E. Crisman, *Integrated Circuits: Chemical and Physical Processing of Integrated Circuits* (American Chemical Society, Washington, DC, 1985).
[2] H. Shang, K.-L. Lee, P. Kozlowski, C. D'Emic, I. Babich, E. Sikorski, M. Ieong, H.-S. P. Wong, K. Guarini, and W. Haensch, IEEE Electron Device Lett. **25**, 135 (2004).
[3] H. Jiang and R. G. Elliman, IEEE Trans. Electron Devices **43**, 97 (1996).
[4] Y. Maeda, Phys. Rev. B **51**, 1658 (1995).
[5] M. Zacharias and P. M. Fauchet, Appl. Phys. Lett. **71**, 380 (1997).
[6] A. Nakajima, T. Futatsugi, K. Kosemura, T. Fukano, and N. Yokoyama, Appl. Phys. Lett. **70**, 1742 (1997).
[7] L. Guo, E. Leobandung, and S. Y. Chou, Appl. Phys. Lett. **70**, 850 (1997).
[8] D.-W. Kim, Y.-H. Kim, X. Chen, C.-H. Lee, S.-C. Song, F. E. Prins, D.-L. Kwong, and S. Banerjee, J. Vac. Sci. Technol. B **19**, 1104 (2001).
[9] L. K. Bera, W. K. Choi, C. S. Tan, S. K. Samanta, and C. K. Maiti, IEEE Electron Device Lett. **22**, 387 (2001).
[10] A. G. Entringer, R. Shinar, and H. R. Shanks, Surf. Sci. **234**, 221 (1990).
[11] P. M. Swearengen, S. J. Davis, and T. M. Niemczyk, Chem. Phys. Lett. **55**, 274 (1978).
[12] M. A. Chowdhury and D. Husain, J. Photochem. **7**, 41 (1977).
[13] M. A. Chowdhury and D. Husain, J. Photochem. **10**, 277 (1979).
[14] J. R. Wiesenfeld and M. J. Yuen, J. Phys. Chem. **82**, 1225 (1978).
[15] A. Fontijn and W. Felder, J. Chem. Phys. **72**, 4315 (1980).
[16] G. Hager, R. Harris, and S. G. Hadley, J. Chem. Phys. **63**, 2810 (1975).
[17] G. A. Capelle and J. M. Brom, Jr., J. Chem. Phys. **63**, 5168 (1975).
[18] Y.-C. Wang, L.-L. Lv, Z.-Y. Geng, G.-L. Dai, D.-M. Wang, and H.-Q. Wang, J. Mol. Struct.: THEOCHEM **724**, 185 (2005).
[19] C. Naulin, M. Costes, Z. Moudden, N. Ghanem, and G. Dorthe, Chem. Phys. Lett. **202**, 452 (1993).
[20] J. Glatthaar, Z.-M. Jiang, and Y.-P. Lee (unpublished).
[21] M. Bahou, K. Sankaran, Y.-J. Wu, Y.-P. Lee, D. Rayner, and B. Simard, J. Chem. Phys. **118**, 9710 (2003).
[22] J.-B. Chou, M. Bahou, Y.-P. Lee, D. Rayner, and B. Simard, J. Chem. Phys. **123**, 054321 (2005).
[23] G. Maier, H. P. Reisenauer, H. Egenolf, J. Glatthaar, and L. Roesch, *Silicon for the Chemical Industry VI Conference*, Loen, Norway, 17–21 June 2002, pp. 285–297.
[24] R. J. Nickles, S. J. Gatley, R. D. Hichwa, D. J. Simpkin, and J. L. Martin, Int. J. Appl. Radiat. Isot. **29**, 225 (1978).
[25] T.-L. Chang, W.-J. Li, G.-S. Qiao, Q.-Y. Qian, and Z.-Y. Chu, Int. J. Mass. Spectrom. **189**, 205 (1999).
[26] M. J. Frisch, G. W. Trucks, H. B. Schlegel *et al.*, GAUSSIAN 03, Revision A.1, Gaussian Inc., Pittsburgh, PA, 2003.
[27] A. D. Becke, J. Chem. Phys. **98**, 5648 (1993).
[28] C. Lee, W. Yang, and R. G. Parr, Phys. Rev. B **37**, 785 (1988).
[29] T. H. Dunning, J. Chem. Phys. **90**, 1007 (1989).
[30] A. D. McLean and G. S. Chandler, J. Chem. Phys. **72**, 5639 (1980).
[31] R. Krishnan, J. S. Binkley, R. Seeger, and J. A. Pople, J. Chem. Phys. **72**, 650 (1980).
[32] J. H. Wood and A. M. Boring, Phys. Rev. B **18**, 2701 (1978).
[33] A. Bergner, M. Dolg, W. Küchle, H. Stoll, and H. Preuß, Mol. Phys. **80**, 1431 (1993).
[34] M. Dolg, *Proceedings of the Effective Core Potentials in Modern Methods and Algorithm in Quantum Chemistry*, NIC Series Vol. 3, 2nd ed., edited by J. Grotendorst (John von Neumann Institute for Computing, Jülich, 2000), p. 507.
[35] X. Wang and L. Andrews, J. Am. Chem. Soc. **125**, 6581 (2003).
[36] X. Wang, L. Andrews, and G. P. Kushto, J. Phys. Chem. A **106**, 5809 (2002).
[37] M. Zhou, L. Jiang, and Q. Xu, J. Phys. Chem. A **109**, 3325 (2005).
[38] L. Zhang, J. Dong, and M. Zhou, J. Chem. Phys. **113**, 8700 (2000).
[39] A. Feltrin, S. N. Cesaro, and F. Ramondo, Vib. Spectrosc. **10**, 139 (1996).
[40] Y.-L. Teng, L. Jiang, S. Han, and Q. Xu, J. Phys. Chem. A **111**, 6225 (2007).
[41] J. S. Ogden and M. J. Ricks, J. Chem. Phys. **52**, 352 (1970).
[42] W. G. Fateley, H. A. Bent, and B. Crawford, Jr., J. Chem. Phys. **31**, 204 (1959).
[43] L. Krim and N. Lacome, J. Phys. Chem. A **102**, 2289 (1998).
[44] See EPAPS supplementary material at http://dx.doi.org/10.1063/1.3236384 for energies, zero-point energies, and relative energies of Ge N_2O isomers (Table SI) and energies and geometries of relevant transition states (Fig. S1) predicted with B3LYP/aug-cc-pVTZ and B3LYP/6-311+G(*d*,*p*).
[45] K. P. Huber and G. Herzberg, Constants of Diatomic Molecules (data prepared by J. W. Gallagher and R. D. Johnson, III) in NIST Chemistry WebBook, NIST Standard Reference Database Number 69, edited by P. J. Linstrom and W. G. Mallard, March 2003, National Institute of Standards and Technology, Gaithersburg, MD 20899 (http://webbook.nist.gov).
[46] M. Chen, A. Zheng, H. Lu, and M. Zhou, J. Phys. Chem. A **106**, 3077 (2002).